Quaternary Science Reviews 198 (2018) 156–170

Contents lists available at ScienceDirect

Quaternary Science Reviews

journal homepage: www.elsevier.com/locate/quascirev

A stratigraphic investigation of the Celtic Sea megaridges based on seismic and core data from the Irish-UK sectors

Edward A. Lockhart [a, *], James D. Scourse [b], Daniel Praeg [c, d, 1], Katrien J.J. Van Landeghem [a], Claire Mellett [e], Margot Saher [a], Louise Callard [f], Richard C. Chiverrell [g], Sara Benetti [h], Colm Ó. Cofaigh [f], Chris D. Clark [i]

[a] School of Ocean Sciences, Bangor University, Menai Bridge, Anglesey, LL59 5AB, UK
[b] College of Life and Environmental Sciences, University of Exeter, Penryn, Cornwall, TR10 9EZ, UK
[c] OGS (Istituto Nazionale di Oceanografia e di Geofisica Sperimentale), Borgo Grotta Gigante, Trieste, Italy
[d] Géoazur (UMR 7329 CNRS), Rue Albert Einstein, 06560 Valbonne, France
[e] Wessex Archaeology, Portway House, Old Sarum Park, Salisbury, Wiltshire SP4 6EB, UK
[f] Department of Geography, Durham University, Lower Mountjoy, South Road, Durham, DH1 3LE, UK
[g] Department of Geography and Planning, University of Liverpool, Liverpool, L69 3BX, UK
[h] School of Geography and Environmental Sciences, Ulster University, Coleraine, Londonderry, BT52 1SA, UK
[i] Department of Geography, Sheffield University, Sheffield, S10 2TN, UK

ARTICLE INFO

Article history:
Received 11 May 2018
Received in revised form
29 August 2018
Accepted 30 August 2018
Available online 10 September 2018

Keywords:
Holocene
Late Pleistocene
Western Europe
Celtic sea
Stratigraphy
Glaciation
Tidal sand ridges
Irish sea ice stream

ABSTRACT

The Celtic Sea contains the world's largest continental shelf sediment ridges. These megaridges were initially interpreted as tidal features formed during post-glacial marine transgression, but glacigenic sediments have been recovered from their flanks. We examine the stratigraphy of the megaridges using new decimetric-resolution geophysical data correlated to sediment cores to test hypothetical tidal vs glacial modes of formation. The megaridges comprise three main units, 1) a superficial fining-upward drape that extends across the shelf above an unconformity. Underlying this drape is 2), the Melville Formation (MFm) which comprises the upper bulk of the megaridges, sometimes displaying dipping internal acoustic reflections and consisting of medium to coarse sand and shell fragments; characteristics consistent with either a tidal or glacifluvial origin. The MFm unconformably overlies 3), the Upper Little Sole Formation (ULSFm), previously interpreted to be of late Pliocene to early Pleistocene age, but here shown to correlate to Late Pleistocene glacigenic sediments forming a precursor topography. The superficial drape is interpreted as a product of prolonged wave energy as tidal currents diminished during the final stages of post-glacial marine transgression. We argue that the stratigraphy constrains the age of the MFm to between 24.3 and 14 ka BP, based on published dates, coeval with deglaciation and a modelled period of megatidal conditions during post-glacial marine transgression. Stratigraphically and sedimentologically, the megaridges could represent preserved glacifluvial features, but we suggest that they comprise post-glacial tidal deposits (MFm) mantling a partially-eroded glacial topography (ULSFm). The observed stratigraphy suggests that ice extended to the continental shelf-edge.

1. Introduction and context

1.1. Celtic Sea megaridges

The Celtic Sea contains an extensive assemblage of shelf-crossing linear ridges, covering an area of ~65,000 km^2 across the Irish, UK and French sectors, with their long axes generally orientated north-east to south-west (Fig. 1; Stride et al., 1982). In the Irish-UK sectors, these are up to 200 km long, 15 km wide, 55 m

* Corresponding author.
E-mail address: edward.lockhart@bangor.ac.uk (E.A. Lockhart).
[1] Currently: Laboratório de Geologia Marinha, Universidade Federal Fluminense, Av. Gen. Milton Tavares de Souza s.n., Gragoatá, Niterói, RJ, 242103–46, BR.

https://doi.org/10.1016/j.quascirev.2018.08.029

high and 20 km apart, and represent the largest examples of such features in the world (Stride et al., 1982). These 'megaridges' are found between depths of −180 m and −100 m. In the French sector of the shelf, the ridges are smaller, existing up to 70 km long, 7.5 km wide, 50 m high and 16 km apart (Bouysse et al., 1976). Early workers argued that the ridges were tidal features, now moribund, formed during lower sea level (Belderson et al., 1986; Bouysse et al., 1976; Stride, 1963; Stride et al., 1982), and it has subsequently been shown that rising post-glacial sea levels were associated with a mega-tidal regime capable of reworking shelf deposits to form ridges (Belderson et al., 1986; Scourse et al., 2009; Uehara et al., 2006; Ward et al., 2016). Alternatively, a possible glacial origin of the ridges was considered by early workers (see Belderson et al., 1986), and has been reconsidered to account for the recovery of glacigenic sediments linked to seismic reflections within the flanks of the megaridges (Praeg et al., 2015a, 2015b).

The Celtic Sea shelf was glaciated by the Irish Sea Ice Stream (ISIS), the offshore extent of which has been constrained by glacigenic sediments on the Isles of Scilly (Scourse, 1991) and in a handful of vibrocores from the Irish and UK sectors (Pantin and Evans, 1984; Praeg et al., 2015b; Scourse et al., 1990). The minimum extent of the ISIS (Sejrup et al., 2005) was reconstructed from the distribution of over-consolidated diamict, Melville Till (MT), recovered at the base of cores on the inner to mid-shelf collected by the British Geological Survey (BGS) in the 1970s and 80s (Scourse et al., 1990). Below water depths of −135 m, the MT gave way to cores of laminated silty clay, Melville Laminated Clay (MLC; Scourse et al., 1990). Both sedimentary facies, MLC overlying MT, were retrieved in BGS vibrocore 49/-09/44 under 2 m of superficial sediment, acquired on the mid-shelf on the flank of a megaridge (Pantin and Evans, 1984), corresponding to Ridge 3 (Fig. 1). Additional glacigenic sediments were recovered from three vibrocores on a megaridge flank, Ridge 5 (Fig. 1), near the shelf-edge and have been interpreted to contain both subglacially deformed sediments and laminated proximal glacimarine sediments containing a bivalve shell dated to 24.3 ka BP, suggesting extension of the ISIS to the shelf-edge during the Last Glacial Maximum (Fig. 1; Praeg et al., 2015b). This shelf-edge age is consistent with dates from the south coast of Ireland, indicating that the initial ice advance occurred after 25–24 ka BP (Ó Cofaigh and Evans, 2007). This advance reached the Isles of Scilly by 25.4–24 ka BP (Smedley et al., 2017) before extending to the shelf-edge and subsequently retreating into St. George's Channel by 24.2 ka BP (Small et al., 2018; Scourse et al., submitted). This chronology suggests that the advance and subsequent retreat of the ISIS across the shelf was rapid (Chiverrell et al., 2013; Ó Cofaigh and Evans, 2007; Scourse et al., submitted; Small et al., 2018).

1.2. Formation of the Celtic Sea megaridges: tidal sand banks vs glacifluvial eskers

Tidal models of the Celtic Sea megaridges have been based on observations of their morphology and internal character, and modelling of shelf conditions during lower sea levels. Seismic profiles across the Celtic Sea ridges reveal dipping and truncated internal reflection surfaces (Pantin and Evans, 1984; Reynaud et al., 1999b), while short (mainly <5 m) sediment cores obtained from the megaridges across the Irish-UK sectors show that the primary unit comprising the ridges, the Melville Formation (MFm), mainly consists of medium to coarse sand and gravel (Evans, 1990; Pantin and Evans, 1984). Huthnance (1982a, 1982b) proposed a mechanism for ridge growth based upon the interaction between bottom friction over a mound and tidal currents, resulting in ridge growth through deposition on the crest and lateral migration. This is different to the mechanism of Houbolt (1968), who suggested that longitudinal helical vortices either side of a mound can result in axial ridge growth with little lateral migration. Tidal ridges generally consist of medium sand with some bedding planes (Davis and Balson, 1992) which transition to an underlying lag deposit at the base of the ridge (Houbolt, 1968), similar to observations of the MFm by Pantin and Evans (1984). Tidal modelling investigations support the interpretation that the Celtic Sea ridges are constructional features formed during rising sea level by strong tidal currents following deglaciation ca. 21 ka BP (Belderson et al., 1986; Scourse et al., 2009; Uehara et al., 2006; Ward et al., 2016), with the energy required to transport coarse sand (Ward et al., 2015). Palaeotidal model results presented in Scourse et al. (2009) suggest that the northern limit of the ridge field could represent the boundary where bed stresses weakened ~10 ka BP, resulting in the features becoming moribund with no additional axial growth.

However, a post-glacial tidal formation of the megaridges conflicts with the presence of glacigenic sediments on their flanks, including laminated and/or stiff fine-grained sediment, from the mid- and outer-shelf (Praeg et al., 2015b; Scourse et al., 1990, submitted). Additionally, gravel and bounders have been recovered from the flanks of ridges across the Irish-UK sectors, with the presence of the former being suggested to represent a mantle of ice-rafted debris (Pantin and Evans, 1984). The presence of glacigenic sediments overlying the ridges and the recovery of MT and MLC in core 49/-09/44 on a megaridge flank, was interpreted to indicate that the MFm existed prior to deglaciation (Evans, 1990; Pantin and Evans, 1984). The observation that glacigenic sediments appear to drape the megaridge flanks in the Irish-UK sectors has been attributed to either partial glacial overriding of the mid-shelf ridges (Scourse et al., 1990) or to tidal ridges forming syngenetically with deglaciation (Scourse et al., 2009). Alternatively, the entire internal bulk of the megaridges could represent large glacifluvial features or giant eskers (Praeg et al., 2015a). The large-scale internal cross-bedding and sandy composition of the MFm, as well as the presence of stiff glacigenic sediments, could be consistent with the characteristics of eskers (Praeg et al., 2015a). Eskers may also be hundreds of kilometers long and up to 80 m high, but commonly have widths <150 m that are consistent with a single subglacial meltwater conduits (e.g. Banerjee and McDonald, 1975; Rust and Romanelli, 1975; Storrar et al., 2015). However, eskerine ridges with widths of kilometres also occur (e.g. Banerjee and McDonald, 1975; Mäkinen, 2003; Rust and Romanelli, 1975), including features up to 10 km wide (Noormets and Flodén, 2002; Veillette, 1986). Large ridges have been attributed to deposition from multiple conduits supplying sediment to over- and backlapping outwash fans along a receding ice margin (Rust and Romanelli, 1975). A time-transgressive origin can account for esker networks >100 km long within a receding ice-marginal zone, producing linear ridge segments with spacings of up to 19 km (Storrar et al., 2014). Eskers are highly variable in structure and lithology, but generally contain several metres of plane- and cross-bedded sand and gravels (Banerjee and McDonald, 1975; Brennand and Shaw, 1996; Gorrell and Shaw, 1991; Hebrand and Åmark, 1989; Mäkinen, 2003). Additionally, eskers may contain a core of boulders and cobbles which fine upward and outward from the centre, representing the deposition of finer grained material due to decreasing meltwater pressures in the final stages of development (Gorrell and Shaw, 1991). As eskers develop in ice marginal zones that may also be subaqueous, glaciofluvial sands and gravels may be interlayered with subglacial diamicts and both give way laterally to lacustrine or marine muds (Rust and Romanelli, 1975).

1.3. Aims and wider context

The aim of this paper is to present new information on the Celtic

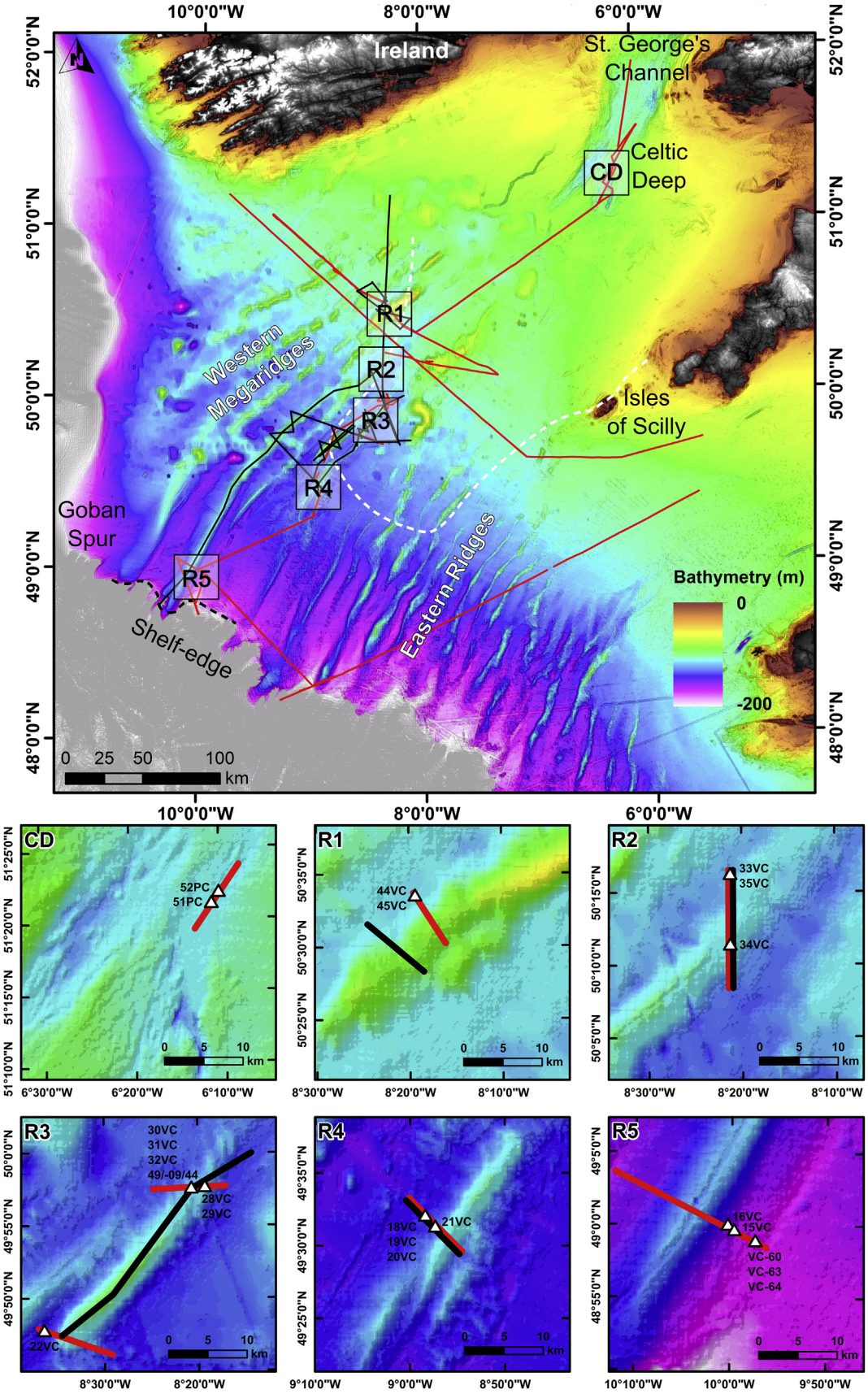

Fig. 1. Map of the Celtic Sea shelf showing shaded regional bathymetry (EMODnet) with topography (Shuttle Radar Topography Mission), Celtic Deep (CD) and various megaridges (R#). The white dashed line shows the minimum extent of subglacial sediments by Scourse et al. (1990) while the black dashed line represents the shelf-edge ice extent suggested by Praeg et al. (2015b). Tracklines show seismic data coverage from the BRITICE-CHRONO cruise (JC-106) in red and additional surveys (CV14007 and GLAMAR) in black. Insets show core and selected seismic line locations referred to in the text.

Sea megaridges, based primarily on high-resolution shallow seismic data and sediment cores acquired in 2014 by the BRITICE-CHRONO project. These data improve our understanding of the stratigraphic context of the sedimentary units composing the megaridges and allow us to test hypothesised tidal and glacial formation mechanisms, providing essential stratigraphic context for glacial sediments of the Celtic Sea.

1.4. Regional stratigraphic setting

The Celtic Sea shelf comprises bedrock outcrops and superficial sediments of Quaternary glacigenic deposits, mud, sand and occasional boulders (Evans, 1990; Hamilton et al., 1980; Pantin and Evans, 1984; Scourse et al., 1990). In contrast, the Celtic Deep, an elongated basin located south of St. George's Channel (Fig. 1), comprises Quaternary sediments up to 375 m thick, interpreted to record deposition during several glaciations (Tappin et al., 1994). The following section summarises the stratigraphic model of the Celtic Sea shelf and Celtic Deep from systematic litho- and seismic-stratigraphic studies by the BGS (Evans, 1990; Pantin and Evans, 1984; Tappin et al., 1994).

Lithostratigraphic units include Layers A and B which form the superficial sediment cover across the shelf. Layer A consists of superficial sand, gravelly sand and muddy sand with thicknesses of up to 2 m in various locations, occasionally forming migratory bedforms (Evans, 1990; Pantin and Evans, 1984; Tappin et al., 1994). Below this is a coarser facies (Layer B) which commonly consists of a basal coarse sand to gravel (Evans, 1990; Pantin and Evans, 1984; Tappin et al., 1994), occasionally containing isolated boulders up to 0.5 m in diameter recovered from the megaridges across the shelf (Pantin and Evans, 1984). Sediment cores recovered across the inner-shelf and from the Celtic Deep show the spatial uniformity of Layer B with an erosional lower boundary, observed as a sharp transition between sedimentary units (Furze et al., 2014). This succession of upper units extends as far north as the Celtic Deep, where laminated silty clays were interpreted to represent glacial deposition in quiet aqueous conditions, and are overlain by Layers A and B which have been radiocarbon dated to the late stages of post-glacial marine transgression (Furze et al., 2014; Scourse et al., 2002). On the inner-shelf and in the Celtic Deep, Layer B contains ages ranging from 13.9 to 4 ka BP, the oldest age being obtained from the Celtic Deep, and is interpreted as extensively reworked (Furze et al., 2014) while Layer A has been dated in the Celtic Deep to the last ~13 ka BP (Scourse et al., 2002). These two layers are found across the Celtic Sea shelf (Evans, 1990; Furze et al., 2014; Pantin and Evans, 1984; Tappin et al., 1994) and overlie glacigenic deposits of the ISIS (Scourse et al., 1990).

Underlying Layers A and B, a single unit, the MFm, was identified across the shelf, corresponding to the bulk of the ridges. Based on seismic data, the MFm is inferred to predominantly consist of sand and is imaged to generally exhibit cross-bedding and other complex internal structures (Pantin and Evans, 1984). It has also been noted that the MFm appears to mantle earlier deposits (Marsset et al., 1999; Pantin and Evans, 1984), suggested to have acted as a nucleus for ridge development. In places, the MFm is suggested to contain glacigenic sediments (Pantin and Evans, 1984), as recovered in core 49/-09/44 where both MLC and MT facies are found (Scourse et al., 1990). These studies inferred the MT and MLC to lie at the top of the MFm, while an exact relationship of these glacigenic sediments to the megaridges has not previously been determined. However, the correlation of core 49/-09/44 to recently acquired seismic data suggests that the MT corresponds to an identifiable reflection extending across the cored mid-shelf megaridge (Praeg et al., 2015a). On the outer-shelf, correlation of short cores to seismic data suggests that glacigenic sediments lie within the seabed refection and may extend across the surface of the megaridge (Praeg et al., 2015b).

The Upper Little Sole Formation (ULSFm) was identified from seismic data to exist below the MFm on the outer-shelf, separated by a typically strong acoustic reflection inferred to represent a coarse lag on its upper surface with channelling at the base of the ULSFm (Pantin and Evans, 1984). A similar acoustic reflection beneath a ridge in the French sector was inferred to have been produced during transgression (Reynaud et al., 1999a). Where this acoustic reflection separating the MFm and ULSFm is not imaged, this is explained by the bounding units having a similar lithology (Pantin and Evans, 1984). In the UK sector, the ULSFm was inferred to consist predominantly of sand with some mud and was sampled by a single vibrocore recovered between megaridges on the outer-shelf, the base of which encountered a muddy sand containing an abundant foraminiferal assemblage interpreted to indicate a Late Pliocene or Early Pleistocene age and record marine deposition (Evans and Hughes, 1984; Pantin and Evans, 1984).

2. Materials and methods

2.1. Equipment and data

Seismic reflection data were acquired in 2014 during BRITICE-CHRONO cruise JC-106 on the RRS *James Cook* using a Kongsberg SBP-120 chirp system with a swept frequency of 2.5–6.5 kHz and a vertical resolution of up to ~0.1 ms two-way-time as measured from profiles. Systematic noise was present in most seismic profiles as a continuous ringing of the seafloor and other high-amplitude reflections. Due to the ringing and processing adjustments during acquisition, a direct comparison of acoustic amplitudes between profiles is not possible. Differential GPS positioning and motion correction were achieved through the usage of Applanix POS-MV, Seapath200 and CNAV3050 systems. Additional seismic data were acquired during the 2014 CV14007 cruise of the RV *Celtic Voyager* using a multi-tip Geo-Source 200–400 sparker, and during the 2009 IPY GLAMAR campaign of the RV *OGS Explora* using a Benthos CAP6600 chirp sub-bottom profiler and a Geo-Source 800 multi-tip sparker. While all seismic data were consulted, only the highest quality seismic data are presented here.

Sediment cores (Table 1) were collected using the BGS 6 m vibrocorer (VC) and National Oceanography Centre 12 m piston corer (PC), for which accurate positions on the seafloor were acquired using a Sonardyne Ranger ultra-short baseline system. A handheld shear-vane was used to provide information on the undrained shear strength of the material soon after the cores were split.

2.2. Seismic-core correlation

A sound velocity of 1600 m s^{-1}, the bulk average sound velocity determined from Geotek multi-sensor core logger measurements, was used to convert core depth into two-way-time and produce an indicative core penetration diagram on seismic profiles to aid visual correlation and to plot approximate reflector depths, where resolvable, on core logs. Seismic profiles show insets of core locations, where alternating black and red blocks correspond to 1 m core lengths from the seafloor. Seismic-facies were identified based on bounding reflections of distinct changes in acoustic character. These facies were correlated based on similar acoustic character, geometry and stratigraphic position, and were correlated to regional BGS units (Pantin and Evans, 1984) based on the original descriptions of seismic and sediment core data. Litho-facies were defined based on observed grain size, bounding surfaces and the relative order of similar deposits.

Table 1
Core recovery details for the JC-106 cruise.

Core	Latitude (DD WGS84)	Longitude (DD WGS84)	Depth (m)	Recovery (m)
15VC	48.99202	−9.98281	165	2.17
16VC	48.99945	−10.00358	160	1.68
18VC	49.54034	−8.99374	146	1.86
19VC	49.53904	−8.99170	145	1.62
20VC	49.53232	−8.98568	143	1.52
21VC	49.52230	−8.96623	137	1.40
22VC	49.79488	−8.60675	142	1.28
28VC	49.96353	−8.31164	125	1.42
29VC	49.96330	−8.31675	122	1.40
30VC	49.96230	−8.33875	124	1.78
31VC	49.96244	−8.33887	125	1.74
32VC	49.96216	−8.34106	125	1.94
33VC	50.27430	−8.34522	132	1.82
34VC	50.18612	−8.35045	118	1.90
35VC	50.27119	−8.34521	130	2.63
44VC	50.56035	−8.32173	125	2.02
45VC	50.56020	−8.32172	125	2.17
51PC	51.34570	−6.18433	116	6.29
52PC	51.36627	−6.16656	116	7.58

3. Results

We present results from sediment cores correlated to seismic profiles on and adjacent to the megaridges at six sites of interest across the shelf (Fig. 1). This allows the identification of nine litho-facies (LFs) identified from 19 sediment cores (Fig. 2) and seven seismic-facies (SFs) identified from seismic profiles (Figs. 3–5) which are then integrated within three shelf-wide stratigraphic units (Table 2), building on the regional framework proposed during BGS mapping based on similar methods (Evans, 1990; Pantin and Evans, 1984; Tappin et al., 1994).

3.1. Litho-facies

LF9 is the only facies cored below LF8 and consists of medium to coarse sand with shell fragments which displays a fining-upward trend to fine sand. LF8 consists of stiff (shear strengths of up to 165 kPa) clay and silt which generally contain fine to medium sand laminations that can in places exhibit deformation, e.g. 33VC (Fig. 2). At Ridge 5, LF8 is similar but has a sandier composition. These sediments were recovered from the lower flanks of the megaridges and generally were not penetrated entirely. At Ridge 1, LF8 was penetrated and is up to 80 cm thick. LF7 comprises medium to coarse sand, occasionally with abundant shell fragments which were recovered on the flank of Ridge 4 and not penetrated entirely. At Ridge 3, LF6 is recovered as coarse sand which contains shell fragments and some clasts. LF5 is a medium to coarse sand at its base and sometimes displays subtle fining-upward grain size trends and bedding planes, recovered from Ridges 2, 3 and 5. LF4 is a massive soft (undrained shear strengths up to 35 kPa) clay found in the Celtic Deep underlying LF3. LF3 was cored as a 1.6 m thick soft mud unit with fine sand laminations and was only recovered in the Celtic Deep. LF2 consists of a coarse layer underlying LF1 which consists of medium sand to gravel with shell fragments and some clasts in shelf cores. This layer is generally <40 cm thick across the shelf. LF2 overlies older deposits, observed as the sharp transition between grain sizes, and appears uniform across the shelf apart from the inclusion of some clasts at Ridge 2. LF1a is only recovered in the Celtic Deep where it exists as a distinct shell fragment layer less than 10 cm thick at the base of LF1 muds. Overlying LF1a and LF2, LF1 represents sediments comprising the present day seafloor. These sediments display fining-upward medium sand to clay, or as a mud or medium sand unit with no observable grain size trend. LF1 has thicknesses exceeding 3 m in isolated depressions such as the Celtic Deep, but is generally <1 m thick across the shelf and megaridges. LF1 sediments sometimes display a coarsening upslope trend, as seen in Ridge 2 cores, with the inter-ridge troughs containing finer-grained sediments in comparison to coarser sediment on the upper megaridge surfaces.

3.2. Seismic-facies

SF7, imaged at Ridge 4 and Ridge 3, rests upon a sub-horizontal reflection and has an upper surface forming positive features within the megaridges (Figs. 4 and 5). In the case of Ridge 3, SF7 comprises low to medium amplitude internal reflections which downlap the lower boundary (Fig. 4) compared to SF7 at Ridge 4, which transitions from having few internal reflections at its base to having a more complex appearance near the top of the unit (Fig. 5). SF6, imaged at Ridge 5 and Ridge 2, consists of positive features similar to SF7, but contains sub-horizontal low to medium amplitude reflections which become discontinuous towards the top of the unit and appear truncated against the upper surface. The upper surface of SF6 is irregular towards the midpoint of the megaridges and rises noticeably on the extreme lateral flanks of the unit to form plateaux (Figs. 3 and 5). SF5, imaged at Ridge 1, has an upper surface which appears sub-horizontal and gently undulating and a lower surface which is highly irregular, while the internal character of the unit appears of low amplitude (Fig. 3). SF4 comprises the upper unit of the investigated megaridges across the shelf, with an upper surface forming mounds (Figs. 3–5). This unit can contain complex reflection geometries, generally including clinoforms which sometimes cross the unit throughout its thickness, e.g. Ridge 1 (Fig. 3). In one instance, Ridge 3 Line E (Fig. 4), SF4 displays subtle evidence of channelling in its uppermost section. SF3 is a low amplitude unit which is found between layers of SF2 in the Celtic Deep (Fig. 3). SF2 consists of beds of high frequency and medium to high amplitude reflections appearing as sub-parallel and wavy parallel which are visibly truncated against the lower boundary of SF1 (Fig. 3). SF1 comprises the uppermost seafloor and is generally of low amplitude in depressions such as the Celtic Deep (Fig. 3). On the shelf, SF1 drapes the megaridges and inter-ridge troughs, varying laterally in thickness, amplitude and continuity (Figs. 3–5). SF1 commonly appears low amplitude in troughs and becomes discontinuous and of medium amplitude upslope, in places filling depressions in the upper surface of SF1.

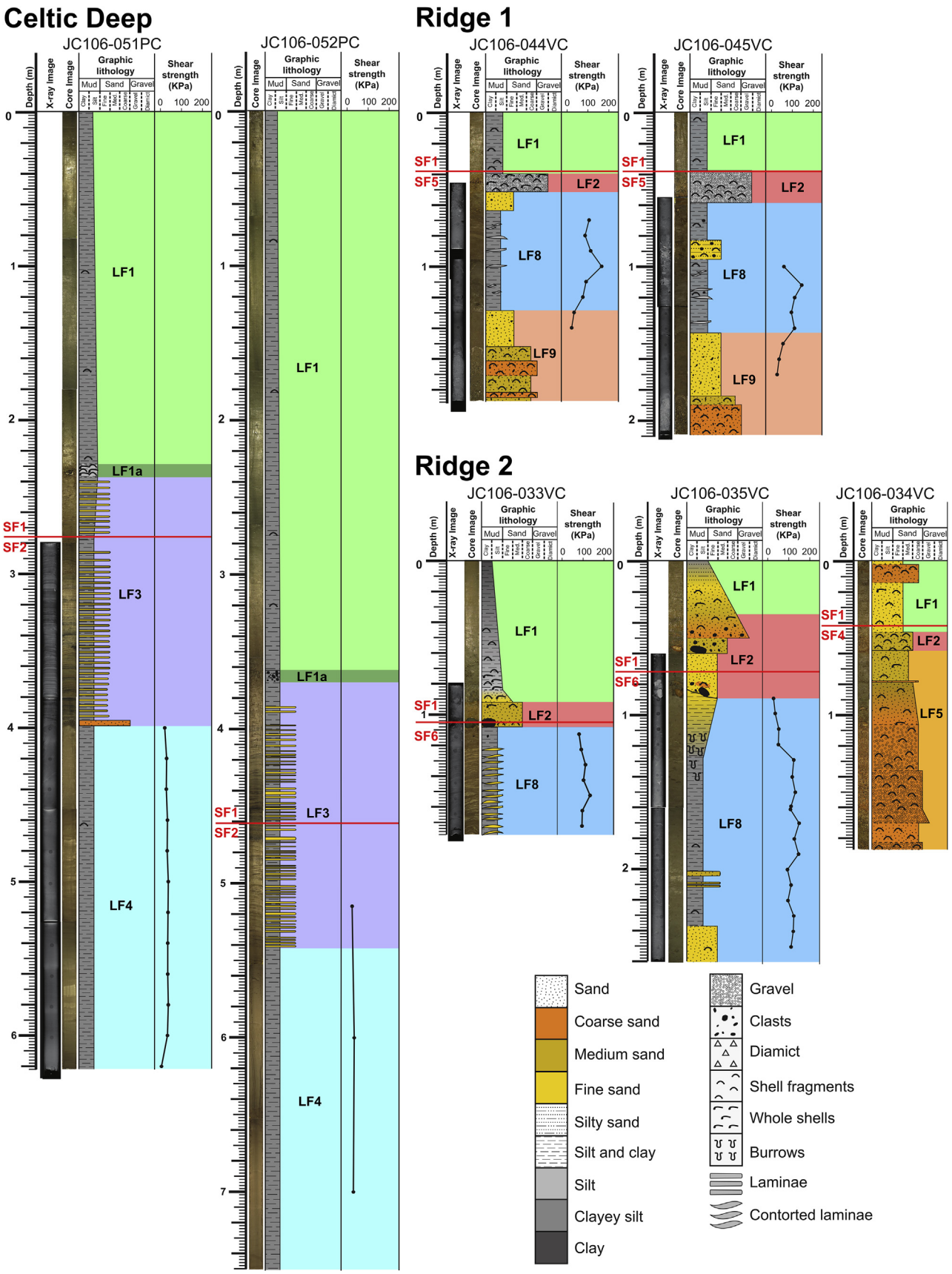

Fig. 2. Lithostratigraphic logs of sediment cores with approximate reflector depths, where resolvable, shown in red using an assumed velocity of 1600 m s^{-1}. See Fig. 1 for core locations.

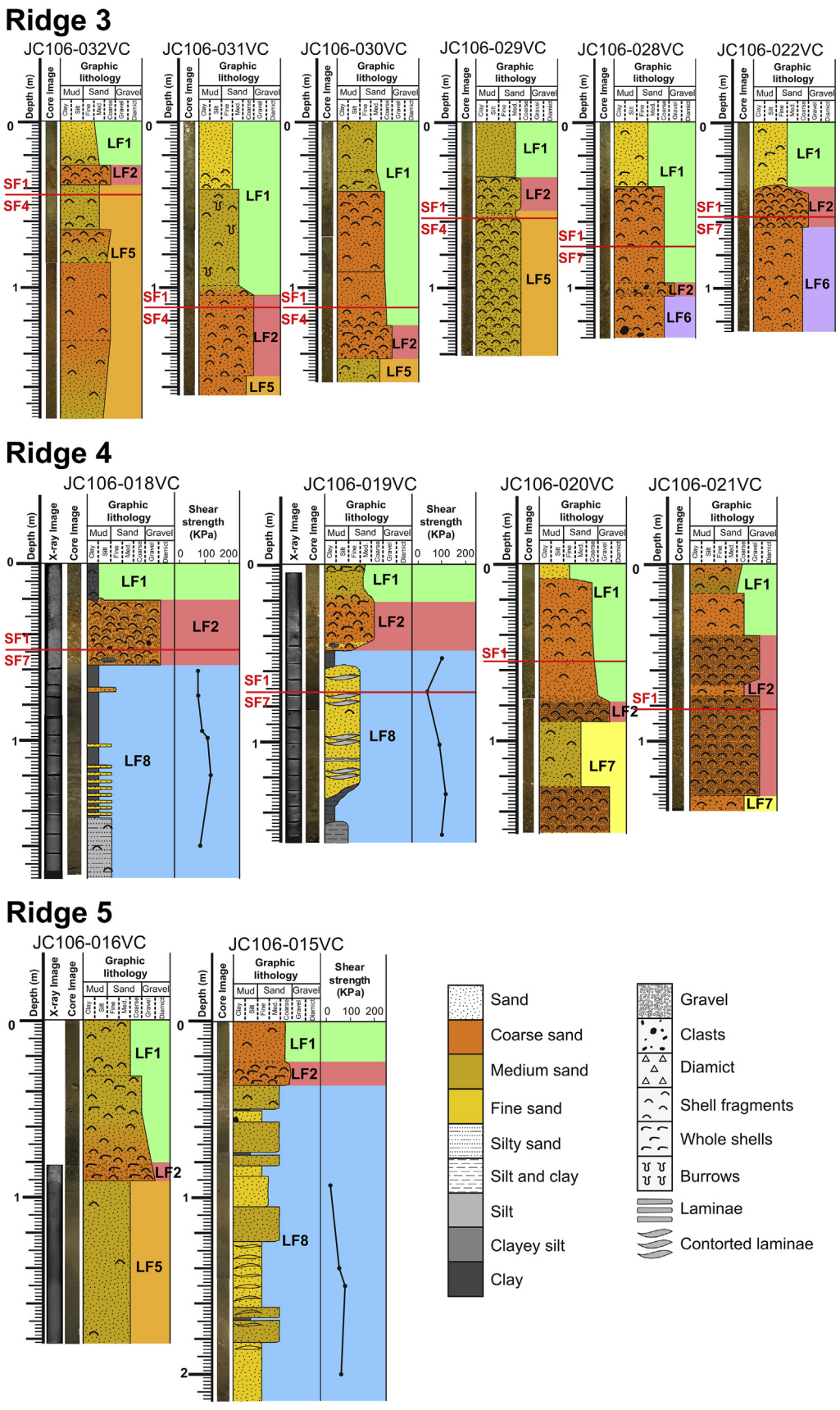

Fig. 2. (*continued*).

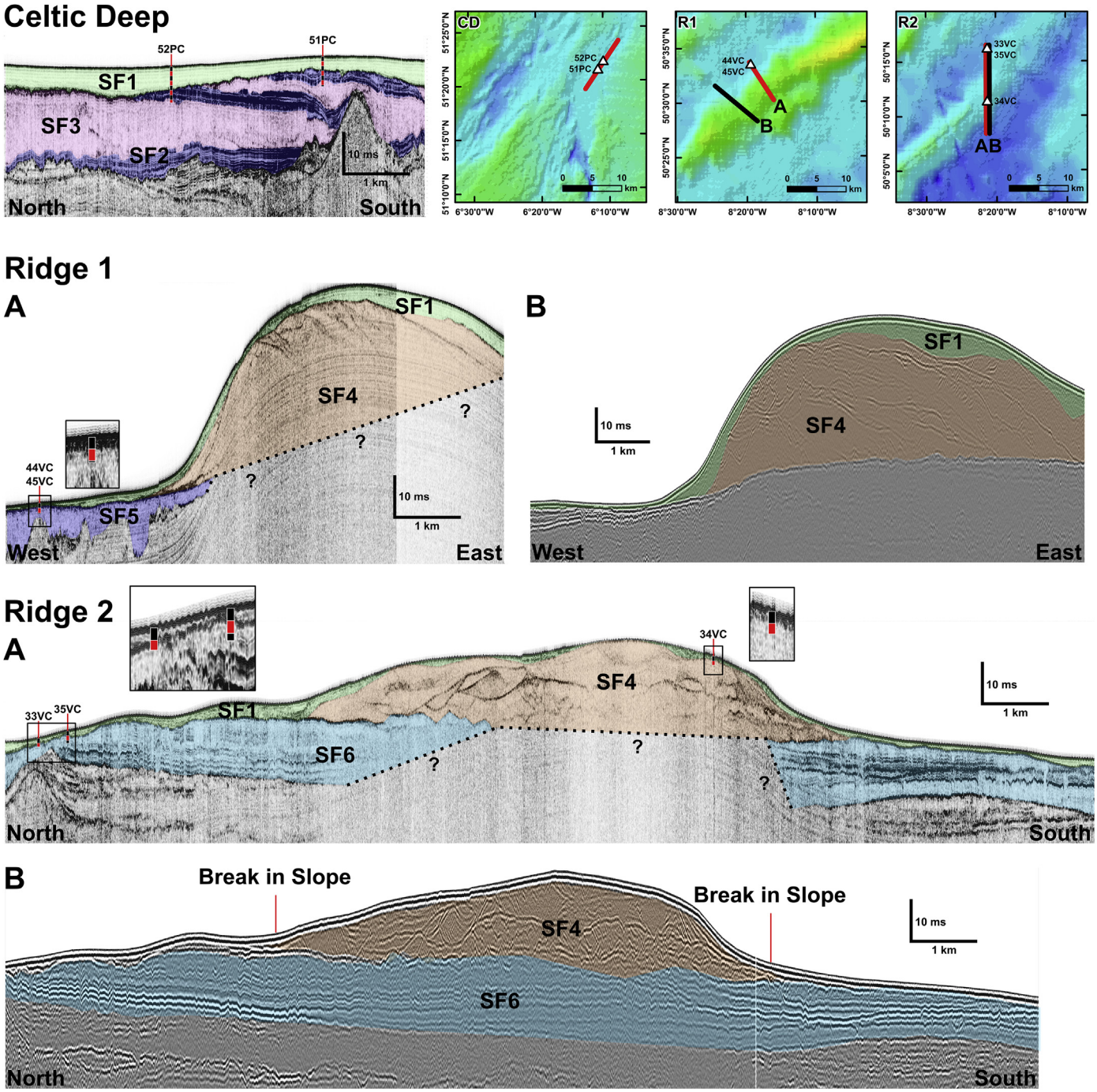

Fig. 3. Seismic-facies of the Celtic Deep based on chirp data, and Ridge 1 and Ridge 2 from chirp (A) and sparker (B) data along the same transects for each megaridge. See Fig. 1 for line and inset locations.

3.3. Regional stratigraphic units

The litho- and seismic-stratigraphic results reveal the presence of several main units comprising the megaridges, which we correlate to the main units identified during BGS mapping (Table 2) based on the original descriptions produced by Pantin and Evans (1984). These units are: 1) a superficial drape, in most areas comprising a fining-upward succession which we correlate to layers A and B and identify for the first time as a seismically resolved unit; 2) the Melville Formation (MFm), a sandy unit corresponding to the bulk of the megaridges; and 3) the Upper Little Sole Formation (ULSFm), which we show to be composed of glacigenic sediments and comprise a lower megaridge unit. These results show that the megaridges consist of three stacked units, rather than a single unit as proposed by Pantin and Evans (1984).

3.3.1. Superficial drape

This seafloor unit drapes the megaridges and older deposits across the shelf, and in most areas is represented by a distinct seismic unit up to several metres thick (SF1) that corresponds in cores to a fining-upward succession with a coarser basal layer. At the seafloor, the composition of SF1 varies laterally, but generally

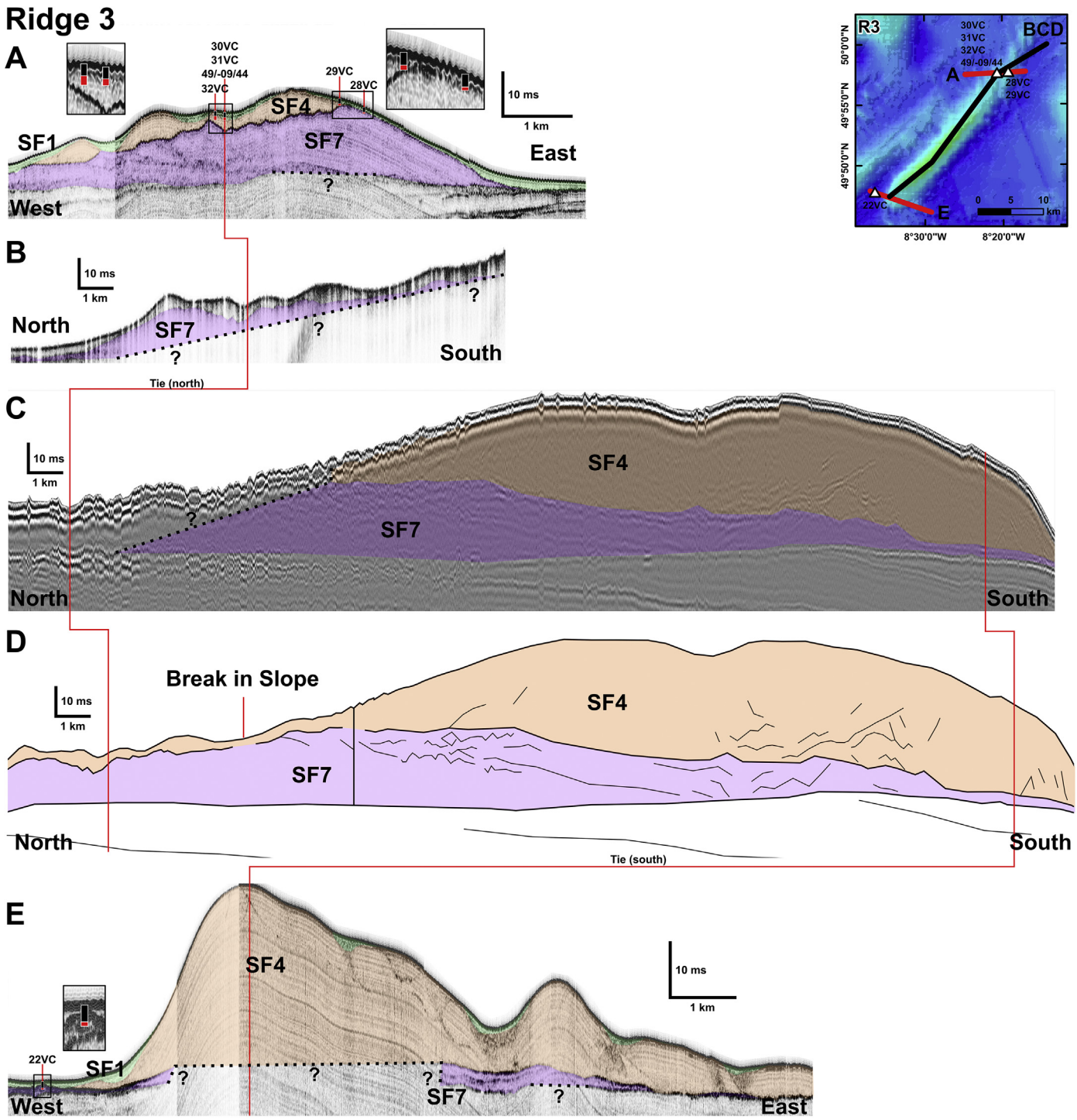

Fig. 4. Seismic-facies based on chirp (A, B and E) and sparker (C) data of Ridge 3 with D showing the combination of B and C along the crest with the merge point marked. See Fig. 1 for line and inset locations.

consists of fine mud and sand in the inter-ridge depressions and the Celtic Deep, and medium to coarse sand upslope from the mega-ridge flanks. SF1 varies in thickness, in places thinning below the resolution of seismic data. A discontinuous seafloor seismic unit was also noted in places by Pantin and Evans (1984), who were unable to define a regional unit corresponding to Layers A and B in cores. Here we infer LF1 and LF2 identified in our cores to correspond to Layers A and B of Pantin and Evans (1984), and to Units I and II of Furze et al. (2014). In the Celtic Deep, LF1a, existing as a basal lag, is additionally correlative to Unit II from Furze et al. (2014) and may have a similar origin to LF2.

3.3.2. *Melville formation (MFm)*

Beneath the superficial drape, seismic data show that the megaridges on the mid- and outer-shelf, Ridges 2, 3, 4 and 5 (Fig. 1), mainly comprise two stacked seismic units (Figs. 3–5), although

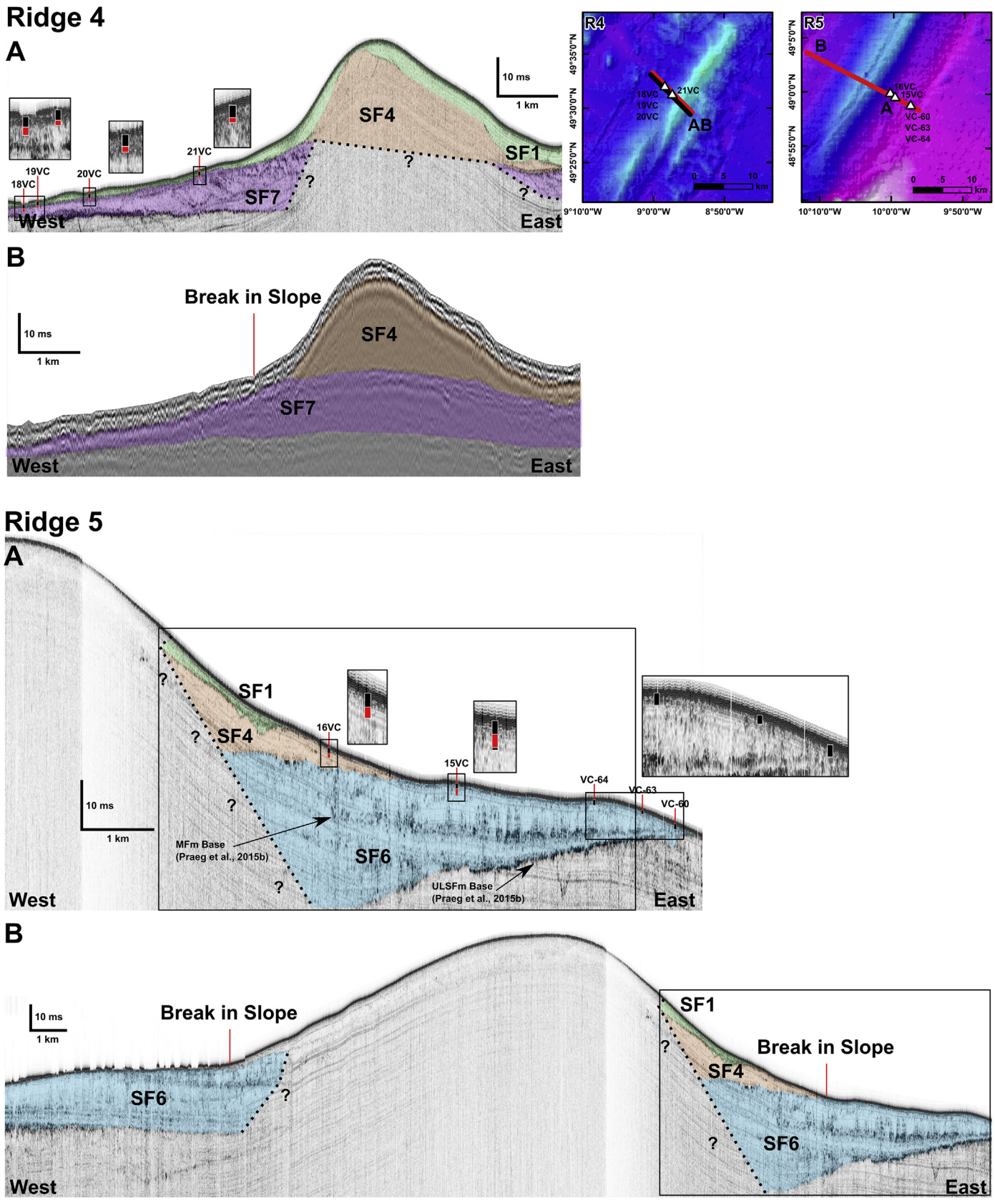

Fig. 5. Seismic-facies based on chirp (A) and sparker (B) data of Ridge 4 and chirp data of Ridge 5 on the eastern flank (A) and across its entire width (B). See Fig. 1 for line and inset locations.

Table 2
Correlation between megaridge stratigraphic units and BGS regional stratigraphic units (Pantin and Evans, 1984).

Ridge Unit	Seismic-facies	Seismic Description	Litho-facies	Lithofacies Description	Age	BGS Unit
Drape	SF1	Superficial drape	LF1	Conformable superficial drape coarsening upslope	<13 ka BP in the Celtic Deep (Scourse et al., 2002)	Layer A
Drape	SF1 (base)	Truncates reflections below	LF1a (Celtic Deep) LF2 (shelf)	Distinct coarse layer with basal unconformity	<14 ka BP in the Celtic Deep (Furze et al., 2014)	Layer B
Upper	SF4	Positive bank with clinoforms	LF5	Medium to coarse sand with shell fragments	N/A	Melville Formation
Lower	SF5	Thin unit filling irregular surface	LF8	Stiff and deformed laminated sediments	27-24 ka BP (Scourse et al., submitted)	Upper Little Sole Formation
Lower	SF6	Laminated unit forming a plateau	LF8	Stiff and deformed laminated sediments	27-24 ka BP (Praeg et al., 2015b; Scourse et al., submitted)	Upper Little Sole Formation
Lower	SF7	Mound on a horizontal base	LF8	Stiff and deformed laminated sediments; Possibly correlative to glacigenics in core 49/-09/44	LF8 - 27–24 ka BP (Scourse et al., submitted); Core 49/-09/44 MT & MLC - Late Pleistocene (Scourse et al., 1990)	Upper Little Sole Formation

only a single unit is observed within Ridge 1 on the inner-shelf (Fig. 3). The upper unit correlates to SF4 and comprises the bulk of the megaridges. SF4 forms prominent mounds with seismically-imaged clinoforms and the top of the unit is composed of LF5, medium to coarse sand with shell fragments, consistent with the description of the MFm by Pantin and Evans (1984). The base of the unit is in most places a strong sub-horizontal or slightly dipping reflection, as described by Pantin and Evans (1984), which commonly coincides with an increase in seafloor slope relative to the lower flanks of the megaridge (Figs. 3–5).

Two possible interpretations exist for the position of the base of the MFm in Ridge 5. Our core sites are coincident with those of Praeg et al. (2015b), who identified a high amplitude reflection (indicated with an arrow in Fig. 5) on pinger data, and correlated it to the base MFm reflection resolved at a similar depth ~8 km away on a BGS sparker profile 1978–55. This implies that the laminated and stiff fine sand and mud recovered from vibrocores VC-64, VC-63 and VC-60 (Fig. 5), corresponding to LF8 in this study, form a drape of glacial sediments at the top of the MFm (Praeg et al., 2015b). An alternative interpretation is presented in Fig. 5, based on the correlation of acoustic facies observed in other megaridges. Ridge 5 displays a similar internal configuration to Ridge 2 (Fig. 3), where the base of the MFm forms a sub-horizontal surface overlying SF6 and coincides with breaks in slope. At Ridge 5, a dipping reflection which varies in continuity and amplitude, as also described by Pantin and Evans (1984), is coincident with a seafloor break of slope and can be interpreted to delineate the boundary between SF4 and SF6 (Fig. 5). In Ridge 5, SF4 and SF6 both consist of medium sand at their interface, accounting for the reduced amplitude reflection. The continuous reflection observed by Praeg et al. (2015b) is here suggested to be part of the internal acoustic character of the unit below the MFm (SF6), forming a bed running parallel with the upper boundary of the unit, similar to layering seen within SF6 on the southern flank of Ridge 2 (Fig. 3). This interpretation contrasts with that of Praeg et al. (2015b), in placing the lower boundary of the MFm higher up the flank of Ridge 5. The glacigenic sediments from LF8 and vibrocores VC-64, VC-63 and VC-60 are thus interpreted to come from SF6, which is exposed on the lower megaridge flanks.

3.3.3. *Upper little sole formation (ULSFm)*

Seismic data show that the MFm overlies a unit that is often exposed on the lower megaridge flanks and is stratified in places, described as SF5, SF6 and SF7. These seismic facies are separated from the MFm by a sub-horizontal to slightly dipping reflection which in places truncates underlying reflections. The lower boundary of these facies either exists as an angular unconformity, truncating the Cockburn Formation of Oligocene to Miocene age (Fig. 4; Evans, 1990; Evans and Hughes, 1984), and in places displays channelling, e.g. Ridge 1 (Fig. 3) and Ridge 5 (Fig. 5). The stratigraphic position and internal character of the unit are all consistent with the description of the ULSFm by Pantin and Evans (1984), who interpreted it to be confined to the outer-shelf. At Ridge 5, the lower boundary of the ULSFm identified in this study lies at the same depth as in Praeg et al. (2015b), and all cores recovered from SF6 contain stiff, laminated and fine-grained material, interpreted as glacigenic by Praeg et al. (2015b) and Scourse et al. (submitted).

BGS core 49/-09/44, recovered on the northern flank of Ridge 3 (Fig. 4), recovered 2 m of superficial sand and gravel above glaciaqueous muds (MLC) and subglacial diamict (MT), both of which were originally correlated to the MFm (Scourse et al., 1990). As core 49/-09/44 cannot be accurately positioned due to the use of the Decca Navigator positioning system, the correlation of MT and MLC with seismic facies is tentative. Our seismic profiles suggest the MT may correlate with SF7 while the MLC appears to correlate to SF4 (Fig. 4). Neither facies were recovered in three neighbouring cores, 30VC and 31VC up to 15 m away and core 32VC 160 m away, all recovering LF5 instead under superficial sediments. However, the glacigenic MT and MLC from core 49/-09/44 may correlate to SF7, and thus the ULSFm, given their approximate recovery on the northern flank where the ULSFm is exposed near the seafloor as seen in other megaridges. The pebbly and shelly coarse sand of LF6 at the bottom of cores 28VC and 29VC seems to penetrate SF7, yet is distinctly different to those sediments recovered in core 49/-09/44 and from the ULSFm recovered at other megaridges.

4. Discussion

The results presented here provide new information on sediments of glacial to post-glacial age, sampled within the megaridges across the Irish-UK sectors of the Celtic Sea shelf. This information implies a revision of both the character and the ages of the three main regional stratigraphic units previously identified during mapping by the BGS. In turn, this revised stratigraphic framework allows us to test hypotheses for the formation of the megaridges.

4.1. Age constraints on stratigraphic units

4.1.1. Superficial drape

Published dates of LF1a and LF2, the basal layer of SF1, from 12 cores recovered across the inner-shelf, extending from the Celtic Deep to the northern megaridges, have yielded a wide spread of radiocarbon ages from 13.9 to 4 ka BP obtained from intertidal molluscs (Furze et al., 2014), the oldest of which were obtained from the Celtic Deep. Other published dates show that SF1 in the Celtic Deep has conformable ages from 13 to 3 ka BP (Scourse et al., 2002). This evidence suggests that SF1 is of post-glacial age on the inner-shelf, and records marine deposition during the late stages of transgression towards the Holocene (Furze et al., 2014). On the outer-shelf, the fining-upward character of the unit is consistent with deposition during decreasing energy and rising post-glacial sea level (Pantin and Evans, 1984). No published dates are available of this unit from the mid-to outer-shelf, therefore the age estimate of SF1 beyond the inner-shelf is an inference. However, due to the time-transgressive nature of post-glacial marine transgression, the age of SF1 is expected to become older towards the shelf-edge.

4.1.2. Melville formation (MFm)

No dated materials are available from the Melville Formation. However, the possible age of the unit can be constrained by dates from over- and underlying units. The MFm is unconformably overlain by the superficial drape, deposition of which dates from at least ~14 ka BP on the inner-shelf. The MFm overlies the ULSFm, here shown to contain glacigenic sediments. Across the shelf, these glacigenic sediments have been radiocarbon dated to 27–24.3 ka BP (Praeg et al., 2015b; Scourse et al., submitted).

4.1.3. Upper little sole formation (ULSFm)

The reported Late Pliocene or Early Pleistocene age of the ULSFm by Evans and Hughes (1984) and Pantin and Evans (1984) is inconsistent with Late Pleistocene radiocarbon ages obtained from glacigenic sediments, including LF8, across the shelf (Praeg et al., 2015b; Scourse et al., submitted).

The Late Pliocene to Early Pleistocene age was based on an analysis of foraminifera in muddy sands at the base of a single BGS vibrocore, acquired between ridges on the outer-shelf (Evans and Hughes, 1984). The core correlation to the ULSFm was not illustrated by a seismic profile, which were noted to be of low seafloor resolution (Pantin and Evans, 1984). One possibility is that the one sample used by Evans and Hughes (1984) to constrain the age of the entire ULSFm was recovered from older deposits. Another possibility is that the muddy sand at the base of the core may represent glacigenic sediments, containing reworked foraminifera from older deposits. Here we reinterpret the ULSFm to be of Late Pleistocene glacial age.

4.2. Hypotheses for megaridge formation

4.2.1. Megaridges as post-glacial tidal banks

The oldest age of ~14 ka BP from the superficial drape is consistent with numerical palaeotidal model outputs of the post-glacial marine transgression (Scourse et al., 2009; Ward et al., 2016), showing a time-transgressive landward reduction in tidal bed stress between 16 and 12 ka BP across the Celtic Sea. This modelled reduction in energy suffers from the uncertainties linked to palaeotidal modelling, such as sea level history and ice extent and chronology inaccuracies, but could explain the fining-upward succession from a basal coarse layer observed in the superficial drape. In this context, prior to 16–12 ka BP, energetic tidal conditions during the peak of transgression, commencing at least 21 ka BP (limited by the temporal limit of the model), provide the primary mechanism for the erosion of shelf sediment and the formation of the MFm (Scourse et al., 2009). As tidal currents reduced in intensity, wave action continued to rework the ridges as water depth increased (Reynaud et al., 1999b). Water depths shallower than 145 m, encompassing the upper ridge surfaces across the shelf at present, are exposed to wave action (Reynaud et al., 1999a), preventing the deposition of fine muds which are generally found in the inter-ridge troughs as observed for LF1. Reduced water depths would have resulted in the wave energy envelope encompassing the megaridges and their neighbouring troughs entirely, resulting in winnowing and erosion, before focusing on the upper megaridge surfaces due to rising sea level. This wave erosion surface may have overprinted earlier erosion surfaces, such as the lower boundary reflection of the MFm where it is exposed on the lower megaridge flanks. We speculate that the superficial drape could be interpreted solely as the product of wave action during rising sea level. In this scenario, the basal lag (LF2) could represent a wave erosion surface, being the last high-energy event to occur during transgression before sea-level rose toward its present level, recorded by the fining-upward deposits of LF1.

The fining-upward sequence recovered from the upper part of the MFm may represent the sedimentary expression of the modelled reduction in tidal energy during transgression (Scourse et al., 2009; Ward et al., 2016). Subsequent wave reworking of the megaridge surfaces could explain the origin of LF2 in 34VC (Fig. 2), through wave conditions partially reworking the upper surface of the MFm to produce a coarser cap of comparable shelly medium sand. Wave reworking during lowered sea level could also account for the shelf-wide angular unconformity at the base of the superficial drape, which truncates strata in the Celtic Deep and clinoforms at Ridge 1 (Fig. 3). Such clinoforms are imaged within the MFm at Ridge 1, suggesting that this megaridge was formed through a single mechanism. Palaeotidal model reconstructions show tidal currents had maximum bed stresses generally aligned with the megaridge axes, providing such a mechanism for ridge growth (Scourse et al., 2009). The model outputs suggest that energetic tidal conditions persisted as late as 12 ka BP following deglaciation (Scourse et al., 2009; Ward et al., 2016) and had sufficient energy to erode coarse sand (Ward et al., 2015), which could explain the significant quantity of coarse material comprising the MFm across the shelf. Cores show that the MFm consists of uniform massive shelly medium to coarse sand, similar to sediments associated with tidal bedforms (Davis and Balson, 1992; Houbolt, 1968).

Below the lower boundary of the MFm is a reflection, interpreted to represent a coarse layer and one or more Pleistocene erosion phases (Pantin and Evans, 1984), that in places truncates glacigenic strata of the ULSFm, e.g. Ridge 2 (Fig. 3). This surface may represent the initial regional erosion surface produced during the onset of energetic tidal conditions, as suggested for another Celtic Sea ridge (Reynaud et al., 1999b). The initial erosion surface, preserved under the MFm, would originally have been regionally extensive before being overprinted by subsequent wave reworking during the formation of SF1, possibly merging both erosion surfaces on the lower flanks and inter-ridge troughs into one coarse layer identified as part of Layer B by Pantin and Evans (1984). This can provide an explanation for the gravel to boulder size sediment reported in Layer B by Pantin and Evans (1984), in that boulders were only found on the lower flanks and in the inter-ridge troughs of the megaridges where the original tidal erosion surface erodes into glacial deposits below. Therefore, LF2 in the inter-ridge troughs would represent a polygenetic erosion surface.

The MFm generally overlies positive precursor features of the ULSFm on the mid- and outer-shelf, as suggested by previous observations (Marsset et al., 1999; Pantin and Evans, 1984). The

glacigenic sediments of the ULSFm form a base on which the MFm rests, and represent an extension of the ULSFm further north than suggested by Pantin and Evans (1984). The ULSFm is laterally discontinuous between megaridges, forming isolated mounds which are separated from the MFm by a distinct upper boundary reflection, consistent with the onset of energetic tidal conditions in the post-glacial tidal ridge model. This supports the suggestion that the topography of the partially eroded ULSFm may have influenced the orientation and formation of the MFm (Pantin and Evans, 1984). However, it is also possible that deposition of the MFm and erosion of the underlying ULSFm occurred simultaneously, with erosion being more pronounced in the inter-ridge troughs.

4.2.2. Megaridges as eroded eskers

The sedimentary composition of eskers varies both vertically and laterally, commonly containing a core of boulders and cobbles which fines upward and outward towards bedded sand, representing decreasing meltwater pressure in the later stages of development (Gorrell and Shaw, 1991). Meltwater drainage can result in highly variable internal structures, varying from plane- to cross-bedded (Brennand and Shaw, 1996; Owen, 1997). This is consistent with seismic observations of cross-bedding within the MFm (Figs. 3–5), and with cores from the upper MFm that contain medium to coarse sand with abundant shell fragments, some displaying a fining upward trend (Fig. 2). In addition, eskers can overlie, underlie or contain layers or lenses of subglacial deposits (Banerjee and McDonald, 1975). Thus in the alternative interpretation of Ridge 5 presented by Praeg et al. (2015b), subglacial and glacimarine sediments were interpreted to represent an eroded carapace at the top of a MFm composed mainly of sand. This was similarly interpreted for Ridge 3 by Praeg et al. (2015a) where a strong reflection at the same level as subglacial till at the base of core 49/-09/44 was suggested to also record a glacigenic carapace over the MFm.

As noted previously, the age of the MFm is constrained by other units to lie between 24.3 and 14 ka BP. The erosion event associated with the base of SF1 has an unknown duration, although it occurred at or before ~14 ka BP on the inner-shelf. Therefore, the unconformity could represent the product of energetic tidal conditions during the early stages of the post-glacial marine transgression, as was suggested for ridges in the French sector (Berné et al., 1998), which palaeotidal reconstructions suggest had commenced by 21 ka BP (restricted by a temporal limit of 21 ka BP; Scourse et al., 2009; Ward et al., 2016). This scenario, which suggests that SF1 is older than ~14 ka BP across the shelf, can most simply facilitate the esker model where the features have survived transgression which only produced SF1 and its underlying unconformity. Therefore, if LF2 is dated to the onset of energetic tidal conditions during transgression (>21 ka BP), or deglaciation (~24 ka BP), assuming aqueous conditions allowed for deposition, then this scenario would be consistent with a glacial origin of the MFm.

If the MFm is of glacifluvial origin, it implies that the megaridges largely survived transgression and/or are eroded remnants of what were initially much larger features. Erosion of such pronounced features is likely, as palaeotidal model outputs suggest that transgression lasted for several thousands of years (Scourse et al., 2009; Ward et al., 2016) and was capable of entraining coarse sand (Ward et al., 2015) throughout. The survival of the megaridges is thus surprising, unless they were armoured by the development of a coarse lag which could be represented by LF2 on the upper megaridge surfaces. Additionally, in the glacifluvial scenario of the MFm, the MFm-ULSFm boundary reflection, representing an erosion surface, requires a glacial explanation.

The initial advance of the ISIS into the Celtic Sea occurred after 25–24 ka BP (Ó Cofaigh and Evans, 2007) and ice retreat started from the shelf-edge by at least 24.3 ka BP (Praeg et al., 2015b). The ice margin had reached St. George's Channel by 24.2 ka BP (Small et al., 2018), indicating retreat was rapid (Chiverrell et al., 2013; Small et al., 2018). If the megaridges are of glacifluvial origin, this timing implies the large quantity of sediment comprising the MFm to have been deposited during a short residence time of a few hundred years of the ISIS on the shelf. In contrast, eskers are typically observed to be absent in areas of higher ice flow velocities (Livingstone et al., 2015) and large and continuous esker generation is favoured during a regime of gradual and stable ice retreat (Storrar et al., 2014).

4.3. Evaluation of megaridge formation mechanisms and implications for glaciation

We showed that the MFm is chronologically constrained by over- and underlying units to have formed between 24.3 and 14 ka BP. This coincides with deglaciation of the shelf, and the ensuing main phase of marine transgression which palaeotidal model outputs suggest was characterised by large tidal amplitudes (Scourse et al., 2009; Ward et al., 2016). Therefore, the constraints on the age of the MFm do not unequivocally allow the differentiation between a tidal or glacifluvial origin for the MFm. In addition, the available geophysical and sample data on the internal character of the MFm can be accommodated by both models.

The preservation of the MFm as large glacifluvial ridges surviving a high-energy post-glacial transgression is difficult to explain in relation to palaeotidal models which suggest that energy was sufficient enough to continuously entrain coarse sediment (Ward et al., 2015) for several thousands of years (Scourse et al., 2009; Ward et al., 2016). Additionally, if the MFm formed in the final stages of ice withdrawal from the Celtic Sea, this would represent a significant quantity of glacifluvial sediment being deposited as eskers within a few hundred years. Eskers are generally formed subglacially, yet the MFm is found in the French sector of the Celtic Sea, well outside defined lateral ice limits on the Isles of Scilly (Scourse et al., 1990). Therefore, we suggest that the megaridges are less likely to be preserved eskers, and it is more likely that the MFm represents post-glacial tidal deposits mantling a partially eroded glacial topography comprising the ULSFm.

Caston (1981) suggested that offshore tidal ridges may owe their morphology and orientation to either excess sediment availability in an energetic environment, the remnants of a sheet deposit being preferentially eroded into by high-energy conditions, or an equilibrium state with sediment transport paths in addition to possibly being anchored to an underlying feature. The discontinuous nature of the ULSFm is possibly a result of the high-energy environment modelled to have occurred after the onset of ISIS deglaciation (Scourse et al., 2009; Ward et al., 2016), resulting in the truncation of laterally continuous strata, e.g. SF6 at Ridge 2 (Fig. 3). These laminations suggest that the ULSFm was originally a continuous sheet. Therefore, the recovery of stiff glacigenic sediments from the remaining ULSFm suggests that such sediments were more readily preserved during high-energy conditions while others were eroded. The MFm may have played a protective role, preserving the remains of the underlying ULSFm from further erosion after the onset of MFm deposition, or stiff sediments produced mounds as erosion commenced, which the MFm anchored to during its formation, or both (Fig. 6). In such scenarios, the anchoring of a sand body to an underlying feature can allow ridge growth through the Huthnance (1982a, 1982b) mechanism as tidal currents interact with the raised mound. Therefore, the megaridges may owe their orientation and location to inherited glacial properties reflected by the high undrained shear strength of the sediments, resulting in their preservation as mounds.

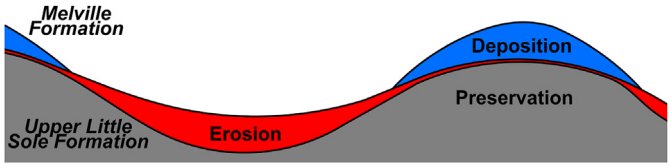

Fig. 6. Schematic cross-section of neighbour megaridges showing alternating areas of erosion and deposition to form preserved mounds of the ULSFm mantled by the MFm.

The occurrence of glacigenic material contributing to the bathymetric expression of the megaridges may explain the contrasting morphology of the smaller ridges on the eastern shelf in comparison to the megaridges displayed here on the western shelf (Fig. 1), and provide insight into the extension of the ISIS. If the revised stratigraphic model presented here is applicable to similar megaridges on the western shelf, then the underlying glacigenic ULSFm, responsible for the large megaridge sizes, may record the extension of the ISIS to the shelf-edge adjacent to the Goban Spur and merge with the shelf-edge limit suggested by Praeg et al. (2015b) and the lateral limit on the Isles of Scilly proposed by Scourse et al. (1990).

5. Conclusions

Correlation of sediment cores with decimetric-resolution seismic data has provided new insight into the glacial to post-glacial stratigraphy of the Celtic Sea shelf and the link between the linear sediment megaridges and glacigenic sediments. Several key findings are revealed:

- Across the shelf, cores recovered glacigenic sediments, consisting of massive or laminated stiff muds, which correlate to the ULSFm where it is exposed on the lower megaridge flanks.
- The ULSFm is thus a Late Pleistocene unit, much younger and more extensive than previously suggested, which forms a precursor glacial topography beneath the investigated megaridges on the mid-to outer-shelf, contributing to their bathymetric expression.
- The overlying MFm forms the bulk of the megaridges and displays internal bedding and comprises massive medium to coarse sand and shell fragments, in places fining-upward, consistent with either a tidal or glacifluvial origin.
- The age of the MFm is constrained by published dates from under- and overlying units to between 24.3 and 14 ka BP, encompassing ice withdrawal from the shelf-edge and the period of strong tidal currents modelled during marine transgression.
- The megaridges and inter-ridge areas are unconformably overlain by a superficial drape consisting of fining-upward deposits of laterally varying character, recording marine deposition over at last the last 14 ka.

It can thus be hypothesised that:

- The undulating topography of the ULSFm in the western Celtic Sea influenced the development, location and orientation of the overlying MFm, and thus the megaridges.
- The MFm is more likely to be of post-glacial tidal origin as it is unclear how glacifluvial landforms could been deposited beyond currently accepted ice limits and during rapid deglaciation of the shelf, or have survived the post-glacial marine transgression if it achieved the modelled duration and intensity.
- The unconformity separating the ULSFm and overlying MFm represents the erosion surface produced during the onset of strong tidal currents associated with the early stages of transgression.
- LF2 represents the product of wave reworking during lowered sea level and diminishing tidal current conditions, overprinting the earlier tidal erosion surface in the inter-ridge areas, while LF1 represents transgressive deposits being reworked by present day conditions on the upper surface of the megaridges.
- As the presence of the ULSFm influences the size of the megaridges, similar megaridges across the western shelf may also contain a core of glacigenic material, with implications for the extension of the ISIS to the western shelf-edge. This glacial legacy can explain the morphological differences between the megaridges of the western glaciated sector and smaller ridges of the eastern non-glaciated sector of the Celtic Sea.

These hypotheses can only be further investigated through similar stratigraphic investigations utilising the integration of high-resolution geophysical data and longer sediment cores of the western megaridges. Further palaeotidal modelling of the Celtic Sea is recommended to include the effect of glacially-influenced bed topography and its evolution in response to energetic conditions during subsequent transgression.

Acknowledgements

This work and E Lockhart were funded by the UK Natural Environment Research Council and the British Geological Survey (Ph.D. studentship 1647721) through the ENVISION doctoral training and Collaborative Awards in Science and Engineering partnerships. Data were acquired during campaigns for the BRITICE-CHRONO project (NERC consortium grant NE/J009768/1), and the OGS project IPY GLAMAR awarded to D Praeg by the Italian polar research agency (PNRA grant 2009/A2.15). D Praeg was further supported by funding from the European Union's Horizon 2020 research and innovation program under Marie Skłodowska-Curie grant agreement No. 656821. The research survey CV14007 was carried out under the Sea Change Strategy with the support of the Marine Institute and the Marine Research Sub-programme of the National Development Plan 2007–2013. We thank the masters, crew and scientists of the RRS *James Cook*, RV *Celtic Voyager* and the RV *OGS Explora*. We thank the reviewers for their comments which have greatly improved this manuscript.

Appendix A. Supplementary data

Supplementary data related to this article can be found at https://doi.org/10.1016/j.quascirev.2018.08.029.

References

Mäkinen, J., 2003. Time-transgressive deposits of repeated depositional sequences within interlobate glaciofluvial (esker) sediments in Köyliö, SW Finland. Sedimentology 50, 327–360. https://doi.org/10.1046/j.1365-3091.2003.00557.x.

Banerjee, I., McDonald, B.C., 1975. Nature of esker sedimentation. In: Jopling, A.V., McDonald, B.C. (Eds.), Glacifluvial and Glaciolacustrine Sedimentation, vol. 23. SPEM Special Publication, Tulsa, Okla, pp. 132–154.

Belderson, R.H., Pingree, R.D., Griffiths, D.K., 1986. Low sea-level tidal origin of Celtic Sea sand banks - evidence from numerical modelling of M2 tidal streams. Mar. Geol. 73, 99–108. https://doi.org/10.1016/0025-3227(86)90113-1.

Berné, S., Lericolais, G., Marsset, T., Bourillet, J.F., De Batist, M., 1998. Erosional offshore sand ridges and lowstand shorefaces: examples from tide- and wave-dominated environments of France. J. Sediment. Res. 68, 540–555. https://doi.org/10.2110/jsr.68.540.

Bouysse, P., Horn, R., Lapierre, F., Le Lann, F., 1976. Étude des grands bancs de sable du sud-est de La mer celtique. Mar. Geol. 20, 251–275.

Brennand, T.A., Shaw, J., 1996. The Harricana glaciofluvial complex, Abitibi region, Quebec: its genesis and implications for meltwater regime and ice-sheet

dynamics. Sediment. Geol. 102, 221–262. https://doi.org/10.1016/0037-0738(95)00069-0.
Caston, G.F., 1981. Potential gain and loss of sand by some sand banks in the Southern Bight of the North Sea. Mar. Geol. 41, 239–250. https://doi.org/10.1016/0025-3227(81)90083-9.
Chiverrell, R.C., Thrasher, I.M., Thomas, G.S.P., Lang, A., Scourse, J.D., Van Landeghem, K.J.J., Mccarroll, D., Clark, C.D., Ó Cofaigh, C., Evans, D.J.A., Ballantyne, C.K., 2013. Bayesian modelling the retreat of the Irish Sea Ice Stream. J. Quat. Sci. 28, 200–209. https://doi.org/10.1002/jqs.2616.
Davis, R.A., Balson, P.S., 1992. Stratigraphy of a North Sea tidal sand ridge. J. Sediment. Petrol. 62, 116–121. https://doi.org/10.1306/D42678A2-2B26-11D7-8648000102C1865D.
Evans, C.D.R., 1990. United Kingdom offshore Regional Report: the Geology of the Western English Channel and its Western Approaches.
Evans, C.D.R., Hughes, M.J., 1984. The Neogene succession of the south western approaches, Great Britain. J. Geol. Soc. 141, 315–326.
Furze, M.F.A., Scourse, J.D., Pieńkowski, A.J., Marret, F., Hobbs, W.O., Carter, R.A., Long, B.T., 2014. Deglacial to postglacial palaeoenvironments of the Celtic Sea: lacustrine conditions versus a continuous marine sequence. Boreas 43, 149–174. https://doi.org/10.1111/bor.12028.
Gorrell, G., Shaw, J., 1991. Deposition in an esker, bead and fan complex, Lanark, Ontario, Canada. Sediment. Geol. 72, 285–314. https://doi.org/10.1016/0037-0738(91)90016-7.
Hamilton, D., Sommerville, J.H., Stanford, P.N., 1980. Bottom currents and shelf sediments, southwest of Britain. Sediment. Geol. 26, 115–138.
Hebrand, M., Åmark, M., 1989. Esker formation and glacier dynamics in eastern Skåne and adjacent areas, southern Sweden. Boreas 18, 67–81. https://doi.org/10.1111/j.1502-3885.1989.tb00372.x.
Houbolt, J.J.H.C., 1968. Recent sediments in the southern bight of the North Sea. Geol. Mijnbouw 47, 245–273.
Huthnance, J.M., 1982a. On the formation of sand banks of finite extent. Estuar. Coast Shelf Sci. 15, 277–299. https://doi.org/10.1017/S0022112006009256.
Huthnance, J.M., 1982b. On one mechanism forming linear sand banks. Estuar. Coast Shelf Sci. 14, 79–99.
Livingstone, S., Storrar, R., Stokes, C., Clark, C., Tarasov, L., Hillier, J., 2015. An ice-sheet scale comparison of diagnosed subglacial drainage routes with esker networks. Geomorphology 246, 104–112. https://doi.org/10.1016/j.geomorph.2015.06.016.
Marsset, T., Tessier, B., Reynaud, J.-Y., De Batist, M., Plagnol, C., 1999. The Celtic Sea banks: an example of sand body analysis from very high-resolution seismic data. Mar. Geol. 158, 89–109. https://doi.org/10.1016/S0025-3227(98)00188-1.
Noormets, R., Flodén, T., 2002. Glacial deposits and ice-sheet dynamic in the north-central Baltic Sea during the last deglaciation. Boreas 31, 362–377. https://doi.org/10.1111/j.1502-3885.2002.tb01080.x.
Ó Cofaigh, C., Evans, D.J.A., 2007. Radiocarbon constraints on the age of the maximum advance of the british-Irish ice sheet in the Celtic Sea. Quat. Sci. Rev. 26, 1197–1203. https://doi.org/10.1016/j.quascirev.2007.03.008.
Owen, G., 1997. Origin of an esker-like ridge - erosion or channel-fill? Sedimentology of the monington “esker” in southwest Wales. Quat. Sci. Rev. 16, 675–684. https://doi.org/10.1016/S0277-3791(97)00015-2.
Pantin, H.M., Evans, C.D.R., 1984. The Quaternary history of the central and south-western Celtic Sea. Mar. Geol. 57, 259–293.
Praeg, D., McCarron, S., Dove, D., Ó Cofaigh, C., Monteys, X., Coxon, P., Accettella, D., Cova, A., Facchin, L., Romeo, R., Scott, G., 2015a. Submarine Geomorphology of the Celtic Sea - New Observations and Hypotheses for the Glaciation of a Mid-latitude continental Shelf. European Geosciences Union Conference Poster.
Praeg, D., McCarron, S., Dove, D., Ó Cofaigh, C., Scott, G., Monteys, X., Facchin, L., Romeo, R., Coxon, P., 2015b. Ice sheet extension to the Celtic Sea shelf edge at the last glacial maximum. Quat. Sci. Rev. 111, 107–112. https://doi.org/10.1016/j.quascirev.2014.12.010.
Reynaud, J.-Y., Tessier, B., Berné, S., Chamley, H., Debatist, M., 1999a. Tide and wave dynamics on a sand bank from the deep shelf of the Western Channel approaches. Mar. Geol. 161, 339–359. https://doi.org/10.1016/S0025-3227(99)00033-X.
Reynaud, J.-Y., Tessier, B., Proust, J.-N., Dalrymple, R., Marsset, T., De Batist, M., Bourillet, J.-F., Lericolais, G., 1999b. Eustatic and hydrodynamic controls on the architecture of a deep shelf sand bank (Celtic Sea). Sedimentology 46, 703–721. https://doi.org/10.1046/j.1365-3091.1999.00244.x.
Rust, B.R., Romanelli, R., 1975. Late Quaternary subaqueous outwash deposits near Ottawa, Canada. In: Jopling, A.V., McDonald, B.C. (Eds.), Glaciofluvial and Glaciolacustrine Sedimentation, vol. 23. SPEM Special Publication, pp. 177–192.
Scourse, J.D., 1991. Late Pleistocene stratigraphy and palaeobotany of the Isles of scilly. Phil. Trans. Roy. Soc. 334, 405–448.
Scourse, J.D., Saher, M., Van Landeghem, K.J.J., Lockhart, E.A., Purcell, C., Callard, L., Roseby, Z.A., Allinson, B., Pieńkowski, A.J., O' Cofaigh, C., Praeg, D., Chiverrell, R.C., Moreton, S., Fabel, D., Clark, C.D., submitted. Advance and Retreat of the Marine-terminating Irish Sea Ice Stream into the Celtic Sea during the Last Glacial: Timing and Maximum Extent, Mar. Geol.
Scourse, J.D., Austin, W.E.N., Bateman, R.M., Catt, J.A., Evans, C.D.R., Robinson, J.E., Young, J.R., 1990. Sedimentology and micropalaeontology of glacimarine sediments from the central and southwestern Celtic Sea. Geol. Soc. Lond. Spec. Publ. 53, 329–347. https://doi.org/10.1144/GSL.SP.1990.053.01.19.
Scourse, J.D., Austin, W.E.N., Long, B.T., Assinder, D.J., Huws, D., 2002. Holocene evolution of seasonal stratification in the Celtic Sea: refined age model, mixing depths and foraminiferal stratigraphy. Mar. Geol. 191, 119–145. https://doi.org/10.1016/S0025-3227(02)00528-5.
Scourse, J., Uehara, K., Wainwright, A., 2009. Celtic Sea linear tidal sand ridges, the Irish Sea Ice Stream and the Fleuve Manche: palaeotidal modelling of a transitional passive margin depositional system. Mar. Geol. 259, 102–111. https://doi.org/10.1016/j.margeo.2008.12.010.
Sejrup, H.P., Hjelstuen, B.O., Dahlgren, K.I.T., Haflidason, H., Kuijpers, A., Nygård, A., Praeg, D., Stoker, M.S., Vorren, T.O., 2005. Pleistocene glacial history of the NW European continental margin. Mar. Petrol. Geol. 22, 1111–1129. https://doi.org/10.1016/j.marpetgeo.2004.09.007.
Small, D., Smedley, R.K., Chiverrell, R.C., Scourse, J.D., Ó Cofaigh, C., Duller, G.A.T., McCarron, S., Burke, M.J., Evans, D.J.A., Fabel, D., Gheorghiu, D.M., Thomas, G.S.P., Xu, S., Clark, C.D., 2018. Trough geometry was a greater influence than climate-ocean forcing in regulating retreat of the marine-based Irish-Sea Ice Stream. Geol. Soc. Am. Bull. https://doi.org/10.1130/B31852.1.
Smedley, R.K., Scourse, J.D., Small, D., Hiemstra, J.F., Duller, G.A.T., Bateman, M.D., Burke, M.J., Chiverrell, R.C., Clark, C.D., Davies, S.M., Fabel, D., Gheorghiu, D.M., McCarroll, D., Medialdea, A., Xu, S., 2017. New age constraints for the limit of the british–Irish ice sheet on the Isles of scilly. J. Quat. Sci. 32, 48–62. https://doi.org/10.1002/jqs.2922.
Storrar, R.D., Stokes, C.R., Evans, D.J.A., 2014. Morphometry and pattern of a large sample (>20,000) of Canadian eskers and implications for subglacial drainage beneath ice sheets. Quat. Sci. Rev. 105, 1–25. https://doi.org/10.1016/j.quascirev.2014.09.013.
Storrar, R.D., Evans, D.J.A., Stokes, C.R., Ewertowski, M., 2015. Controls on the location, morphology and evolution of complex esker systems at decadal timescales, Breidamerkurjökull, southeast Iceland. Earth Surf. Process. Landforms 40, 1421–1438. https://doi.org/10.1002/esp.3725.
Stride, A.H., 1963. north-east trending ridges of the Celtic Sea. Proc. Ussher Soc. 1, 62–63.
Stride, A.H., Belderson, R.H., Kenyon, N.H., Johnson, M.A., 1982. Offshore tidal deposits: sand sheet and sand bank facies. In: Stride, A.H. (Ed.), Offshore Tidal Sands: Processes and Deposits. Chapman & Hall, New York, pp. 95–125.
Tappin, D.R., Chadwick, R.A., Jackson, A.A., Wingfield, R.T.R., Smith, N.J.P., 1994. United Kingdom offshore Regional Report: the Geology of Cardigan Bay and the Bristol Channel.
Uehara, K., Scourse, J.D., Horsburgh, K.J., Lambeck, K., Purcell, A.P., 2006. Tidal evolution of the northwest European shelf seas from the Last Glacial Maximum to the present. J. Geophys. Res.: Oceans 111, 1–15. https://doi.org/10.1029/2006JC003531.
Veillette, J.J., 1986. Former southwesterly ice flows in the Abitibi - timiskaming region: implications for the configuration of the late Wisconsian ice sheet. Can. J. Earth Sci. 23, 1724–1741.
Ward, S.L., Neill, S.P., Van Landeghem, K.J.J., Scourse, J.D., 2015. Classifying seabed sediment type using simulated tidal-induced bed shear stress. Mar. Geol. 367, 94–104. https://doi.org/10.1016/j.margeo.2015.05.010.
Ward, S.L., Neill, S.P., Scourse, J.D., Bradley, S.L., Uehara, K., 2016. Sensitivity of palaeotidal models of the northwest European shelf seas to glacial isostatic adjustment since the Last Glacial Maximum. Quat. Sci. Rev. 151, 198–211. https://doi.org/10.1016/j.quascirev.2016.08.034.